

# Photoplastic near-field optical probe with sub-100 nm aperture made by replication from a nanomould

G. M. KIM\*, B. J. KIM†‡, E. S. TEN HAVE†, F. SEGERINK†,  
N. F. VAN HULST† & J. BRUGGER\*

\*Microsystems Laboratory, Ecole Polytechnique Fédérale de Lausanne (EPFL), 1015 Lausanne, Switzerland

†MESA Research Institute, University of Twente, The Netherlands

**Key words.** Microfabrication, nanomould, NSOM, self-assembled monolayer, SU-8.

## Summary

Polymers have the ability to conform to surface contours down to a few nanometres. We studied the filling of transparent epoxy-type EPON SU-8 into nanoscale apertures made in a thin metal film as a new method for polymer/metal near-field optical structures. Mould replica processes combining silicon micromachining with the photo-curable SU-8 offer great potential for low-cost nanostructure fabrication. In addition to offering a route for mass production, the transparent pyramidal probes are expected to improve light transmission thanks to a wider geometry near the aperture. By combining silicon MEMS, mould geometry tuning by oxidation, anti-adhesion coating by self-assembled monolayer and mechanical release steps, we propose an advanced method for near-field optical probe fabrication. The major improvement is the possibility to fabricate nanoscale apertures directly on wafer scale during the microfabrication process and not on free-standing tips. Optical measurements were performed with the fabricated probes. The full width half maximum after a Gaussian fit of the intensity profile indicates a lateral optical resolution of  $\approx 60$  nm.

## Introduction

Since the first aperture-type near-field experiment in the microwave region (Ash & Nicholls, 1972) and in the optical domain (Pohl *et al.*, 1984), the area of application for near-field optical measurements has because they overcome the diffraction limitation of optical resolution when using the far-field method. One of the most reliable probes at present is a tapered single-mode optical fibre probe (Betzig *et al.*, 1991). The end of the fibre is tapered to a tip by heating and pulling,

the tip is subsequently coated with aluminium to create a subwavelength aperture. The drawbacks of these optical fibre tips are insufficient reproducibility and poor homogeneity of both tip fabrication and aperture making. An alternative way to make the tip is to use wet chemical etching (Hoffmann *et al.*, 1995; Stöckle *et al.*, 1999). Chemically etched probes have higher throughput due to a large tip angle, but they suffer from large surface roughness, an asymmetrically shaped apex, and also from problems caused by post metal deposition on the free-standing probes. A fibre-type probe with improved aperture definition using a focused ion beam (FIB) has been shown to have better polarization and image quality (Veerman *et al.*, 1998).

Recently, several studies on microfabricated near-field scanning optical microscopy (NSOM) probes based on atomic force microscopy (AFM) cantilever (Abraham *et al.*, 1998; Eckert *et al.*, 2001) and photoplastic NSOM probes (Genolet *et al.*, 2001; Kim *et al.*, 2001) have been presented.

Here, we present an improved manufacturing process for a photopolymer NSOM probe using a nanomould technique. The major improvement with respect to our previous publication (Kim *et al.*, 2001) is the possibility of fabricating nanoscale apertures directly onto a wafer-scale nanomould during the microfabrication process rather than onto free-standing tips (German Patent, DE19923444.2-42). An integrated approach to making the nanoscale aperture has the potential to reduce fabrication costs.

## Fabrication process

Basically, the fabrication process follows the steps described earlier (Kim *et al.*, 2001) with the essential difference that the apertures are made directly into the metal layer in the mould *before* forming the polymer probe. The probe consists of three parts: a lower aluminium metal layer as an optical blocking layer with a nanometre-scale aperture, the photoplastic main body of the probe, and an optical fibre as a light guide from the laser source to the polymer probe. The upper part of the main

Correspondence: G. M. Kim. Tel.: +41 21 693 6724; fax: +41 21 693 6670; e-mail: gyuman.kim@epfl.ch

‡Present address: School of Mechanical Engineering, Kyungpook National University, 702–701 Daegu, Korea.

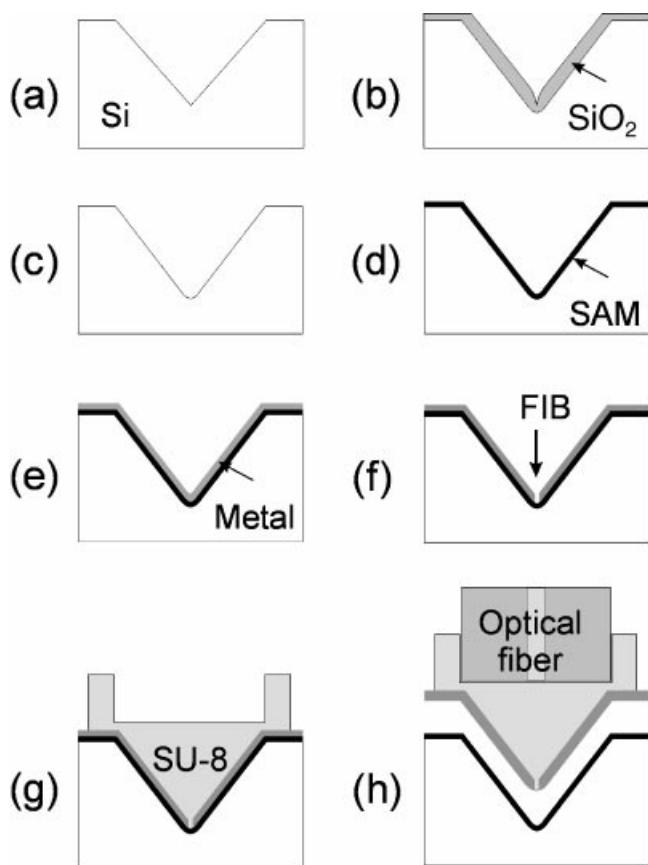


**Fig. 1.** Schematic process diagram of novel SNOM probe fabrication. (a) Inverted tip shape definition on mould. (b) Mould shape control by oxidation. (c) Oxide layer removal (mould rounding). (d) SAM formation. (e) Metal deposition. (f) Nano-aperture opening by FIB. (g) Polymer probe structuring. (h) Optical fibre bonding and releasing from mould.

probe is connected into the optical fibre. The lower side of the probe including the tip is covered with metal except for the tip end with the aperture. The process can be divided briefly into the following steps:

- (a) micromould fabrication for tip shape by KOH etching;
- (b) mould shape control by low temperature oxidation;
- (c) mould rounding with oxide etching;
- (d) coating with a release layer of self-assembled monolayer (SAM);
- (e) deposition of metal (Al) layer;
- (f) opening of nanometre-scale aperture by FIB to form a 'nanomould in the micromould';
- (g) filling the micro- and nanomould with polymer and structuring the upper part of the probe;
- (h) fibre bonding and probe releasing from mould.

Figure 1 shows the details of the fabrication process.

#### Micromould fabrication

Our fabrication sequence started with micromould fabrication in a <100>-orientated p-type 75-mm Si wafer with resistivity

of  $< 10 \Omega \text{ cm}$ . Inverted shapes of pyramidal tips were made on the Si mould by KOH (Merck, 25% wt at 75 °C) wet etching using a 500-nm thick thermal SiO<sub>2</sub> etching mask. In order to make the tip shape with precise radius control, local non-uniform oxide growth at low temperature (Marcus *et al.*, 1990; Alkamine & Quate 1992) was used. This technique is normally used for tip sharpening, but recently we reported its use for controlling the tip radius at the nanometre scale between 10 and 250 nm (Kim *et al.*, 2002b). A 450-nm-thick SiO<sub>2</sub> layer was grown by low temperature wet oxidation at 900 °C for 5 h and removed by BHF in order to make the tip mould round. The rounding defines an opening angle near the tip apex, which is beneficial to the transmission of light near the aperture. Besides that, a round probe is expected to be more robust when operated and scanned near surfaces, and to be able to withstand unexpected collisions into the sample surface. Furthermore, a slightly rounded mould structure makes the mechanical lift-off (see below) more reliable as sharp edges in the mould are known to cause pinholes in the metal film during lift-off.

#### Metal deposition and nanoscale aperture making

A self-assembled monolayer (SAM) of dodecyltrichlorosilane was formed on the mould surface (Kim *et al.*, 2002a) by dipping it into 1 mM solution of dodecyltrichlorosilane in distilled toluene for 4 h. This step forms an ultra-thin (1.5 nm) SAM layer, which is essential to allow for the probe replication without affecting the geometry at a nanometre scale.

A 150-nm thick layer of aluminium was then coated directly onto the SAM layer by e-beam evaporation. The base pressure was  $1 \times 10^{-7}$  mbar and the deposition rate of metal was  $0.4 \text{ nm s}^{-1}$ . This metal layer serves as a light-blocking layer in the fabricated probe.

An aperture of  $100 \times 100 \text{ nm}^2$  was then drilled through the metal layer in the mould using a FIB. Various apertures of sizes down to  $50 \times 50 \text{ nm}^2$  can be made on the metal layer. In earlier studies, direct FIB milling of sub-micrometre scale aperture on free-standing probes were reported (Veerman *et al.*, 1998; Kim *et al.*, 2001). However as the set-up and alignment time for modifying free-standing probes is long, and the number of the loaded probes is limited, those solutions can not be used for cost-efficient mass fabrication. Our new approach to FIB milling at the wafer-scale is advantageous because thousands of holes can be drilled using automatic FIB alignment. Figure 2 shows a typical  $100 \times 100 \text{ nm}^2$  aperture made by FIB drilling in a 150-nm thick Al layer inside the mould.

#### SU-8 structuring and probe releasing

Two layers of SU-8 were then spin coated onto the metal layer with the aperture, and structured by lithography and development. An essential asset of SU-8 here is that the polymer fills the mould and the previously made nano-apertures in the

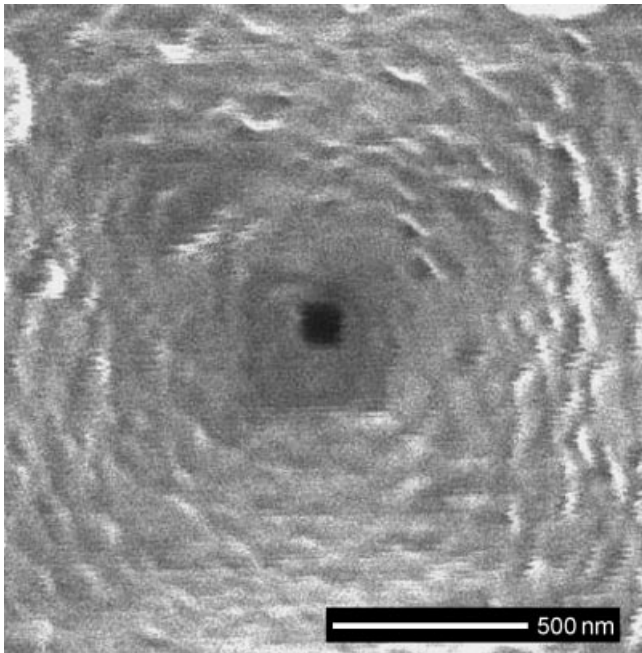


**Fig. 2.** Focused ion beam (FIB) image of aperture made inside the mould. An aperture of  $100 \times 100 \text{ nm}^2$  is drilled through a 150-nm-thick Al layer on the mould by FIB milling. Step (f) in Fig. 1.

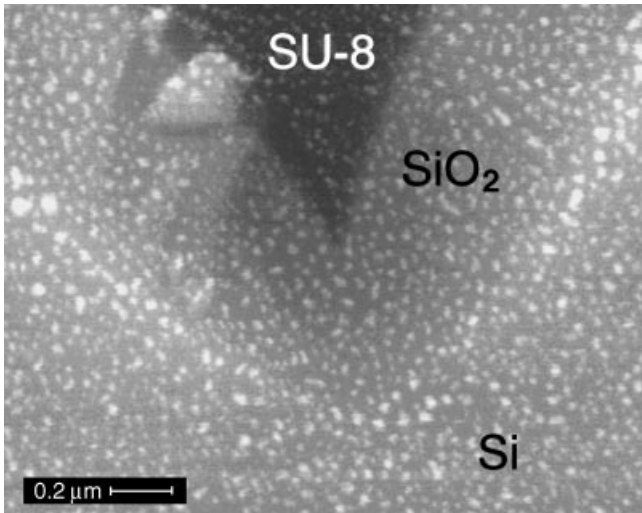


**Fig. 3.** Scanning electron microscopy image of cross-section of V-groove filled with photoplastic SU-8. The SU-8 is fully filled into ultra-sharp mould down to 10 nm range. The white particles on the surface are gold particles coated to prevent charging of SEM images.

aluminium layer. Figure 3 shows a scanning electron microscopy (SEM) image of a cross-section of V-groove filled with SU-8. The SU-8 was fully filled into an ultra-sharp pit in the mould down to the 10 nm range. A cleaved optical fibre was then assembled into the top of the fabricated probe and bonded

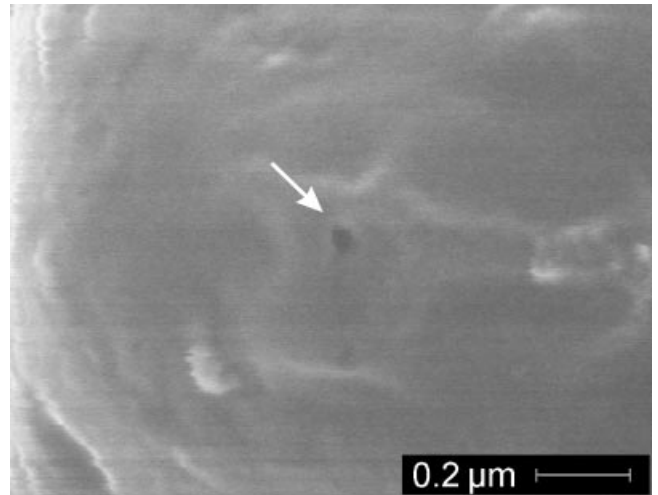
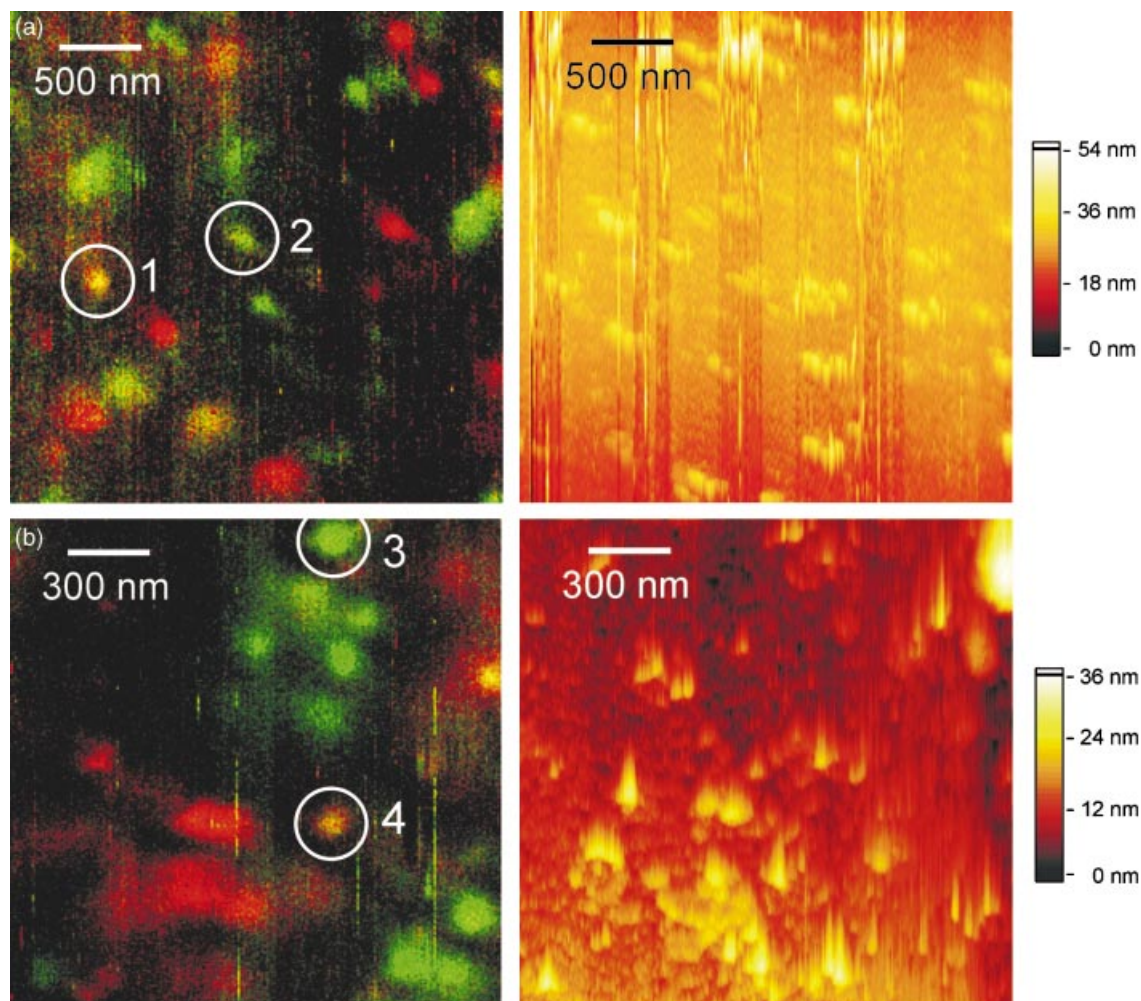


**Fig. 4.** SEM image of aperture on the tip of released SNOM probe. Aperture made on metal layer of mould was released successfully from the mould together with the probe. Step (h) in Fig. 1.

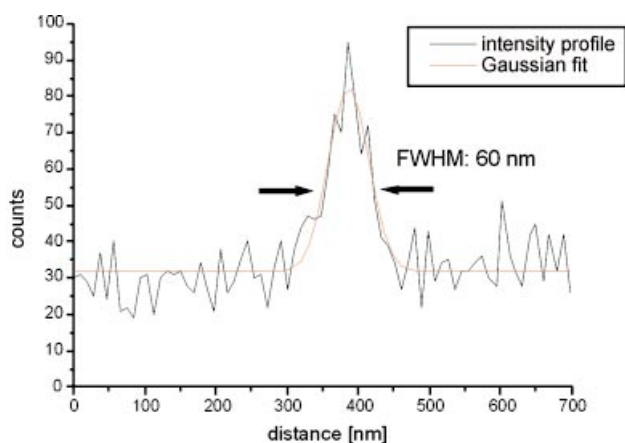
using optical glue under UV light. Finally, the photoplastic probe together with nano-aperture on the light-blocking metal layer was mechanically released from the micro- and nanomould.

Figure 4 shows an SEM image of a NSOM probe released from the mould. The probe was bonded using a tuning fork. Shear-force distance control was used and the probe-to-sample distance is kept below 10 nm (Ruiter *et al.*, 1997b). The enlarged SEM image of the probe tip clearly shows the released aperture. The aperture size was  $\approx 55 \text{ nm}$  although the value on the other side of metal layer was 100 nm, which explains the taper of the aperture.

The fabricated photoplastic probes were then used in a home-built NSOM set-up for polarization sensitive single molecule detection (Ruiter *et al.*, 1997a). The sample consisted of single corbocyanine molecules ( $\text{DiIC}_{18}$ ) in a polymer layer (PMMA) which were excited at 514 nm with typically  $1 \text{ W cm}^{-2}$  excitation power. The fluorescence was collected with a 1.3 NA objective, filtered with a 550 nm long-pass filter, and directed onto two photon-counting avalanche photodiodes by a broadband polarizing beamsplitter, so that two orthogonal polarization directions were detected. Figure 5 shows the fluorescence images obtained with two probes with a 100 nm aperture on the mould; the colour scheme shows the orientation of the molecules (red, vertical direction; green, horizontal direction; yellow, in-between horizontal and vertical) (Veerman *et al.*, 1999). The images show that the probes do not have a preferential direction of polarization for the transmission of light. The typical feature size of the single molecules is  $\approx 100 \text{ nm}$  for both probes (molecules 1, 2 and 3), although certain molecules (e.g. molecule 4) measured with the probe of image 4b are substantially smaller ( $\approx 60 \text{ nm}$ , Fig. 6). The fabricated probes showed better optical resolution



**Fig. 5.** SNOM images of single molecules taken by two fabricated probes. (a) Optical and topography images taken by probe 1 (scanning area  $3 \times 3 \mu\text{m}^2$ ). (b) Optical and topography images taken by probe 2 (scanning area  $1.8 \times 1.8 \mu\text{m}^2$ ). The topography images show the surface of the spin-coated PMMA, and the optical images show the fluorescence of the molecules embedded in the PMMA.



**Fig. 6.** Intensity profile of molecule 4 in Fig. 5(b). The signal-to-noise ratio is  $\approx 2$  and the FWHM of the intensity profile after Gaussian fit is  $\approx 60 \text{ nm}$ .

because the aperture of the released probe was smaller than the expected drilled size due to the taper of the aperture. The optical throughput of the probes is  $8.5 \times 10^{-5}$  and  $4.9 \times 10^{-5}$ , respectively.

### Conclusions

We have demonstrated the microfabrication of NSOM probes using a new nanomould technique. This process has several advantages: first, mass fabrication of probes using an integrated moulding process enables low cost and high reproducibility. Second, the SAM anti-adhesion layer and rounded mould edge allow mechanical releasing of the probe without pinhole formation. The combination of a full mould-scale aperture making process, conformal filling of polymer into the nanomould, and the new releasing method allow low cost and wafer-scale NSOM probe fabrication.

## Acknowledgements

The authors would like to thank J. Huskens and E. Speets for fruitful discussion on the SAM work. This research was financially supported by the Strategic Research Orientation NanoLink of MESA +, University of Twente, and by EPFL.

## References

- Abraham, M., Ehrfeld, W., Lacher, M., Mayr, K., Noell, W., Guthner, P. & Barenz, J. (1998) Micromachined aperture probe tip for multifunctional scanning probe microscopy. *Ultramicroscopy*, **71**, 93–98.
- Akamine, S. & Quate, C.F. (1992) Low-temperature thermaloxidation sharpening of microcast tips. *J. Vacuum Sci. Technol. B*, **10**, 2307–2310.
- Ash, E.A. & Nicholls, G. (1972) *Nature*, **237**, 510.
- Betzig, E., Trautman, J.K., Harris, T.D., Weiner, J.S. & Kostelak, R.L. (1991) Article title. *Science*, **251**, 1468.
- Eckert, R., Freyland, J.M., Gersen, H., *et al.* (2001) Near-field optical microscopy based on microfabricated probes. *J. Microsc.* **202**, 7–11.
- Genolet, G., Despont, M., Vettiger, P., *et al.* (2001) Micromachined photoplastic probe for scanning near-field optical microscopy. *Rev. Sci. Instrum.* **72**, 3877–3879.
- Hoffmann, P., Dutoit, B. & Salathe, R.-P. (1995) Comparison of mechanically drawn and protection layer chemically etched optical fiber tips. *Ultramicroscopy*, **61**, 165–170.
- Kim, B.J., Flamma, J.W., ten Have, E.S., Garcia-Parajo, M.F., van Hulst, N.F. & Brugger, J. (2001) Moulded photoplastic probes for near-field optical applications. *J. Microsc.* **202**, 16–21.
- Kim, G.M., Kim, B.J., Liebau, M., Huskens, J., Reinhoudt, D.N. & Brugger, J. (2002a) Surface modification with self-assembled monolayers for nanoscale replication of photoplastic MEMS. *J. Microelectromech. Syst.* **11**, 175–181.
- Kim, G.M., Kovalgin, A., Holleman, J. & Brugger, J. (2002b) Nanomold radius control by thermal oxidation sharpening and wet etching. *J. Nanoscience Nanotechnol.* **2**, 55–59.
- Marcus, R.B., Ravi, T.S., Gmitter, T., *et al.* (1990) Formation of silicon tips with < 1 nm radius. *Appl. Phys. Lett.* **56**, 236–238.
- Pohl, D.W., Denk, W. & Lanz, M. (1984) Optical sthethoscopy: image recording with resolution 1/20. *Appl. Phys. Lett.* **4**, 651–653.
- Ruiter, A.G.T., Veerman, J.A., Garcia-Parajo, M.F. & van Hulst, N.F. (1997a) Article title. *J. Phys. Chem. A*, **101**, 7318.
- Ruiter, A.G.T., Veerman, J.A., van der Werf, K.O. & van Hulst, N.F. (1997b) Dynamic behavior of tuning fork shear force feedback. *Appl. Phys. Lett.* **71**, 28–30.
- Stöckle, R., Fokas, C., Deckert, V. & Zenobi, R. (1999) High-quality near-field optical probes by tube etching. *Appl. Phys. Lett.* **75**, 160–162.
- Veerman, J.A. *et al.* (1999) *J. Microsc.* **194**, 477.
- Veerman, J.A., Otter, A.M., Kuipers, L. & van Hulst, N.F. (1998) High definition aperture probes for near-field optical microscopy fabricated by focused ion beam milling. *Appl. Phys. Lett.* **72**, 3115–3117.